

QRD-based Precoded MIMO-OFDM Systems With Reduced Feedback

Kyeong Jin Kim, Man-On Pun, Ronald Iltis

TR2010-007 March 2010

Abstract

QR decomposition (QRD)-based precoded MIMO-OFDM systems with reduced feedback are proposed to convert the MIMO-OFDM channel into layered subchannels. QRD-M is further combined with either singular value (SVD) or geometric mean decomposition (GMD) of the time-domain channel impulse response matrix. As a result, the receiver in the proposed systems only needs to feed back information describing one precoding matrix for all carriers. Simulation results confirm the bit-error-rate (BER) and throughput performance superiority of the proposed systems compared to conventional SVD per-carrier precoding schemes.

IEEE Transaction of Communications

This work may not be copied or reproduced in whole or in part for any commercial purpose. Permission to copy in whole or in part without payment of fee is granted for nonprofit educational and research purposes provided that all such whole or partial copies include the following: a notice that such copying is by permission of Mitsubishi Electric Research Laboratories, Inc.; an acknowledgment of the authors and individual contributions to the work; and all applicable portions of the copyright notice. Copying, reproduction, or republishing for any other purpose shall require a license with payment of fee to Mitsubishi Electric Research Laboratories, Inc. All rights reserved.

QRD-based Precoded MIMO-OFDM Systems With Reduced Feedback

Kyeong Jin Kim, Man-On Pun and Ronald A. Iltis

Abstract

QR decomposition (QRD)-based precoded MIMO-OFDM systems with reduced feedback are proposed to convert the MIMO-OFDM channel into layered subchannels. QRD-M is further combined with either singular value (SVD) or geometric mean decomposition (GMD) of the time-domain channel impulse response matrix. As a result, the receiver in the proposed systems only needs to feed back information describing *one* precoding matrix for all carriers. Simulation results confirm the bit-error-rate (BER) and throughput performance superiority of the proposed systems compared to conventional SVD per-carrier precoding schemes.

Index Terms

Orthogonal frequency division multiplexing (OFDM), multiple-input multiple-output (MIMO), geometric mean decomposition (GMD), QR decomposition (QRD), reduced-feedback precoding.

I. INTRODUCTION

Orthogonal Frequency Division Multiplexing (OFDM) has emerged as one of the most promising physical-layer technologies for next-generation wireless communications due to its robustness against frequency-selective fading and high spectral efficiency. Furthermore, the multiple-input multiple-output (MIMO) technology can be employed to further enhance the performance of the OFDM system by exploiting spatial diversity/multiplexing gain. Indeed, MIMO-OFDM has been standardized as the physical-layer technology for IEEE 802.11n, and is currently being considered for IEEE 802.16 and 4G.

K. J. Kim is with Nokia Inc., 6000 Connection Drive, Irving, TX 75039.

M. O. Pun is with Mitsubishi Electric Research Laboratories (MERL), 201 Broadway, Cambridge, MA 02139. This work was done when he was a Croucher post-doctoral fellow at Princeton University, Princeton, NJ.

R. A. Iltis is with the Department of Electrical and Computer Engineering, University of California, Santa Barbara, CA 93106. His work was supported in part by a gift from Nokia.

To fully exploit the advantages provided by MIMO, precoding techniques have been extensively studied in the literature. It is well-known that the singular value decomposition-based precoding scheme (SVD-PCS) with transmission power allocation achieves Shannon Capacity [1]. However, without transmit channel state information (CSI) needed for optimized power allocation, it is known that the performance of SVD-PCS is limited by the spatial subchannel with the lowest signal-to-noise ratio (SNR). The geometric mean decomposition precoding scheme (GMD-PCS) has been proposed to decompose the MIMO channel into identical subchannels with equal power when transmit CSI is unavailable [2]. Despite their good performance in single-carrier systems, SVD-PCS and GMD-PCS are not suitable for MIMO-OFDM systems with a large number of carriers. This is because SVD-PCS or GMD-PCS transmitters must feed back one precoding matrix per carrier [1], [2], leading to prohibitive feedback overhead. Considerable effort has been devoted to developing limited-feedback precoding schemes for MIMO-OFDM [3]–[6]. However, these existing methods require sophisticated quantization schemes to minimize information loss.

In this work, we propose two QRD-based precoding schemes for the MIMO-OFDM system with reduced feedback by employing QRD in conjunction with either SVD or GMD. In contrast to conventional precoded MIMO-OFDM systems where each carrier is precoded with one matrix derived directly from either SVD [1] or GMD [2], the proposed system employs the same precoder for all carriers as derived from a novel layered subchannel decomposition. As a result, only one precoding matrix needs to be computed and fed back to the transmitter. Simulation results confirm the BER and throughput performance of the proposed systems.

Notation: Vectors and matrices are denoted by boldface letters. $\|\cdot\|$ denotes the Frobenius norm of the enclosed matrix. \mathbf{I}_N is the $N \times N$ identity matrix and $\mathbf{A} = \text{diag}\{a_0, a_1, \dots, a_{N-1}\}$ is a diagonal matrix. Finally, we use $(\cdot)^T$ and $(\cdot)^H$ for transposition and Hermitian, respectively.

II. SIGNAL AND CHANNEL MODEL

We consider an N -carrier and K -spatial data stream MIMO-OFDM system equipped with N_r and N_t receive and transmit antennas ($N_r \leq N_t$), respectively. For clarity, we first concentrate on the full-rate system with $K = N_r = N_t$ whereas the partial spatial-rate system with $K = N_r$, $N_r < N_t$ will be highlighted in Sec. V. Since we emphasize reduced-feedback precoding here, adaptive modulation and coding (AMC) is not considered and all data streams are encoded with

the same code parameters. Let $\mathbf{s}_n = [s_n^1, s_n^2, \dots, s_n^K]^T$ with s_n^k being the coded data symbol modulated over the n -th carrier in the k -th data stream for $n = 1, 2, \dots, N$. We use $h_i^{p,q}$ to denote the discrete-time composite channel impulse response of the channel between the p -th transmit antenna and the q -th receive antenna (encompassing the transmit/receive filters and the transmission medium). We consider a slow-fading environment and assume that $h_i^{p,q}$ is constant over the entire transmission interval. Thus, the corresponding channel response vector can be written as $\mathbf{h}^{p,q} = [h_0^{p,q}, h_1^{p,q}, \dots, h_{N_f-1}^{p,q}]^T$, where N_f is the channel order. The CP is assumed to be sufficient to span the maximum path delay. Furthermore, we assume that $\mathbf{h}^{p,q}$ is perfectly known to the receiver.

Consider the samples received by the q -th receive antenna. The received samples are first serial-to-parallel (S/P) converted into data blocks. After CP removal, each data block is converted into the frequency domain using an N -point discrete Fourier transform (DFT) yielding

$$\mathbf{y}_n = \frac{1}{\sqrt{K}} \mathbf{H}_n \mathbf{T}_n \mathbf{s}_n + \mathbf{z}_n, \quad (1)$$

where \mathbf{T}_n is a $K \times K$ unitary precoding matrix, $\mathbf{z}_n = [z_n^1, z_n^2, \dots, z_n^K]^T$ is the frequency-domain Gaussian noise and $\mathbf{H}_n \in \mathbb{C}^{K \times K}$ is the frequency-domain channel response matrix of the n -th carrier given as

$$\mathbf{H}_n = \begin{bmatrix} \mathbf{w}_n^T \mathbf{h}^{1,1} & \dots & \mathbf{w}_n^T \mathbf{h}^{K,1} \\ \vdots & \ddots & \vdots \\ \mathbf{w}_n^T \mathbf{h}^{1,K} & \dots & \mathbf{w}_n^T \mathbf{h}^{K,K} \end{bmatrix}, \quad (2)$$

with $\mathbf{w}_n = [1, e^{-j2\pi n/N}, \dots, e^{-j2(N_f-1)\pi n/N}]^T$.

To facilitate the detection of \mathbf{s}_n from \mathbf{y}_n , the conventional approaches decompose the MIMO channel \mathbf{H}_n into either parallel subchannels using SVD [1] or GMD [2], respectively,

$$\mathbf{H}_n = \mathbf{U}_{H_n} \mathbf{\Lambda}_{H_n} \mathbf{V}_{H_n}^H \quad (\text{SVD-PCS}), \quad (3)$$

$$= \mathbf{B}_{H_n} \mathbf{E}_{H_n} \mathbf{P}_{H_n}^H \quad (\text{GMD-PCS}), \quad (4)$$

where \mathbf{U}_{H_n} , \mathbf{V}_{H_n} , \mathbf{B}_{H_n} and \mathbf{P}_{H_n} are all unitary matrices, $\mathbf{\Lambda}_{H_n}$ is a diagonal matrix and \mathbf{E}_{H_n} is an upper triangular matrix with equal diagonal elements. Subsequently, \mathbf{V}_{H_n} or \mathbf{P}_{H_n} is employed as the precoding matrix for the n -th carrier. Again, we wish to develop a precoder that avoids the carrier-dependence due to \mathbf{H}_n of (3) by using a single matrix for all carriers.

III. QRD/SVD-BASED PRECODING SCHEME

A. Proposed channel decomposition

Rewrite the frequency response channel matrix \mathbf{H}_n shown in (2) as

$$\mathbf{H}_n = [\mathbf{I}_K \otimes \mathbf{w}_n^T] \begin{bmatrix} \mathbf{h}^{1,1} & \dots & \mathbf{h}^{K,1} \\ \vdots & \ddots & \vdots \\ \mathbf{h}^{1,K} & \dots & \mathbf{h}^{K,K} \end{bmatrix} = [\mathbf{I}_K \otimes \mathbf{w}_n^T] \mathbf{H}, \quad (5)$$

where \otimes denotes the Kronecker product. Eq. (5) indicates that \mathbf{H}_n is a product of a carrier dependent matrix and carrier independent matrix $\mathbf{H} \in \mathbb{C}^{(N_f K) \times K}$. Thus, we can decompose the MIMO channel matrix \mathbf{H}_n using SVD as follows.

$$\mathbf{H}_n = [\mathbf{I}_K \otimes \mathbf{w}_n^T] [\mathbf{U}_H \mathbf{\Lambda}_H \mathbf{V}_H^H], \quad (6)$$

where $\mathbf{U}_H \in \mathbb{C}^{N_f K \times K}$ and $\mathbf{V}_H \in \mathbb{C}^{K \times K}$ are unitary matrices while $\mathbf{\Lambda}_H \in \mathbb{C}^{K \times K}$ is a diagonal matrix with entries $\lambda_{H,1} \geq \lambda_{H,2} \geq \dots \geq \lambda_{H,K}$.

Substituting the QRD of $[\mathbf{I}_K \otimes \mathbf{w}_n^T] \mathbf{U}_H = \mathbf{Q}_{n,U} \mathbf{R}_{n,U}$ into (6), where $\mathbf{Q}_{n,U} \in \mathbb{C}^{K \times K}$ and $\mathbf{R}_{n,U}$ are unitary and upper triangular respectively, we have

$$\mathbf{H}_n = \mathbf{Q}_{n,U} \mathbf{R}_{n,\Lambda} \mathbf{V}_H^H, \quad (7)$$

where $\mathbf{R}_{n,\Lambda} \triangleq \mathbf{R}_{n,U} \mathbf{\Lambda}_H \in \mathbb{C}^{K \times K}$ is also upper-triangular.

Thus, the common precoding matrix \mathbf{V}_H is applied to all carriers by the transmitter. The receiver then uses the unitary matrix $\mathbf{Q}_{n,U}$ as part of the detector/decoder. Since the precoding scheme proposed in (7) employs SVD followed by QRD, it is referred to as the QRD/SVD precoding scheme (QRD/SVD-PCS) in the sequel.

Two comparisons between QRD/SVD-PCS and the existing schemes merit further comments. First, albeit the similarity between (7) and SVD-PCS and GDM-PCS shown in (3), the precoding matrix in QRD/SVD-PCS, \mathbf{V}_H , is *not* a function of the carrier index. Second, it is straightforward to show that the computational complexity of the proposed QRD/SVD-PCS is $\mathcal{O}((N+2)K^3)$ and on a par with that of SVD-PCS for a large N .

B. Precoding matrix selection

Ideally, \mathbf{V}_H can be perfectly fed back to the transmitter and employed as the precoder. In practice, \mathbf{V}_H must be quantized to minimize overhead. Thus, a common codebook of 2^B precoding matrices is shared by the transmitter and receiver. After computing \mathbf{V}_H , the receiver selects

a precoding matrix $\mathbf{T}^{(j)}$ that best matches \mathbf{V}_H and then returns the index $j \in \{1, 2, \dots, 2^B\}$. We choose a precoder $\mathbf{T}^{(j)}$ that minimizes the mean squared error (MSE) between the transmitted and received symbols over all carriers :

$$j^* = \arg \min_{j \in \{1, \dots, 2^B\}} \|\mathbf{V}_H^H \mathbf{T}^{(j)} - \mathbf{I}_K\|^2. \quad (8)$$

Again, we emphasize that the quantization (8) is independent of the carrier index, whereas separate quantizations for each carrier are required in the conventional SVD-PCS method.

C. Data detection

Assuming $\mathbf{T}^{(j)}$ has been selected as the precoding matrix, detection of s_n from the received signal \mathbf{y}_n is next considered. The received signal precoded by $\mathbf{T}^{(j)}$ can be expressed as

$$\mathbf{y}_n^{(j)} = \frac{1}{\sqrt{K}} \mathbf{Q}_{n,U} \mathbf{R}_{n,\Lambda} \mathbf{I}_K s_n + \tilde{\mathbf{z}}_n, \quad (9)$$

where we have defined

$$\tilde{\mathbf{z}}_n \triangleq \frac{1}{\sqrt{K}} \mathbf{Q}_{n,U} \mathbf{R}_{n,\Lambda} (\mathbf{V}_H^H \mathbf{T}^{(j)} - \mathbf{I}_K) s_n + \mathbf{z}_n. \quad (10)$$

If the non-Gaussian quantization noise is assumed to have sufficiently smaller power than \mathbf{z}_n , we can approximate $\tilde{\mathbf{z}}_n$ as Gaussian distributed with the zero mean and covariance given by

$$\mathbf{R}_{\tilde{\mathbf{z}}_n} = \frac{1}{K} \mathbf{Q}_{n,U} \mathbf{R}_{n,\Lambda} \mathbf{A} \mathbf{A}^H \mathbf{R}_{n,\Lambda}^H \mathbf{Q}_{n,U}^H + \frac{2N_0}{T_s} \mathbf{I}_K, \quad (11)$$

where $\mathbf{A} = \mathbf{V}_H^H \mathbf{T}^{(j)} - \mathbf{I}_K$.

It has been shown in [7] that the QRD-M algorithm is an effective receiver structure for reliable data detection over layered subchannels. Here we use the soft-QRD-M data detector developed in [7]. Let $c_{n,\ell}^k = (\mathbf{c}_n^k)_\ell$ be the ℓ -th binary source bit mapped to s_n^k , for $\ell = 1, 2, \dots, L$. In particular, $L = 2$ stands for the QPSK modulation scheme. Assuming $p(c_{n,\ell}^k = 1) = p(c_{n,\ell}^k = -1)$, the log-likelihood-ratio (LLR) of each source bit can be approximated by

$$\hat{L}(c_{n,\ell}^k) \approx \ln \frac{\hat{p}(c_{n,\ell}^k = 1 | \mathbf{y}_n^{(j)})}{\hat{p}(c_{n,\ell}^k = -1 | \mathbf{y}_n^{(j)})} = \ln \frac{p(\mathbf{y}_n^{(j)} | c_{n,\ell}^k = 1)}{p(\mathbf{y}_n^{(j)} | c_{n,\ell}^k = -1)} + \lambda_2(c_{n,\ell}^k). \quad (12)$$

Furthermore, $\lambda_2(c_{n,\ell}^k)$ is the log a-posteriori probability (log-APP) generated by the channel decoder. Thus, the likelihood can be further expressed as

$$p(\tilde{\mathbf{y}}_n^{(j)} | c_{n,\ell}^k = \pm 1) = \sum_{\substack{c_{n,\gamma}^i = \pm 1 \\ (\gamma,\nu) \neq (\ell,k)}} \prod_{p=1}^K \exp \left\{ -\frac{1}{2N_0/T_s} \left| [\tilde{\mathbf{y}}_n^{(j)}]_p - \sum_{i=p}^K [\mathbf{R}_{n,\Lambda}]_{p,i} \cdot s_n^i(c_{n,i}^i) \right|^2 \right\}, \quad (13)$$

where $\tilde{\mathbf{y}}_n^{(j)} = \mathbf{Q}_{n,U}^H \mathbf{y}_n^{(j)}$. The upper triangular matrix $\mathbf{R}_{n,\Lambda}$ leads to a tree structure for the sum-product term in (13) and the prior APP $\lambda_2(c_{n,\ell}^k)$, with $(2^L)^k$ branches at level k for $k = 1, \dots, K$. The decoder extrinsic can be incorporated into the soft-QRD-M detector to improve its performance. The sum-product at each level of the tree is then approximated by a sum over the K -largest partial likelihoods as described in [7]. Iterative decoding as in [8] is employed, with $\lambda_2(c_{n,\ell}^k) = 0$ on the first pass of the QRD-M algorithm. The likelihoods in (13) are then used by the decoder to generate new extrinsics $\lambda_2(c_{n,\ell}^k) \neq 0$.

IV. QRD/GMD-BASED PRECODING SCHEME

It is well-known that the overall BER performance of MIMO systems is usually dictated by the spatial subchannel with the lowest SNR. Since QRD/SVD-PCS decomposes the MIMO channel into *layered* subchannels, a simple closed-form solution for the power allocation cannot be obtained even when transmit CSI is available. Rather than directly allocating transmission power to different spatial channels, we propose to exploit the GMD technique developed in [2]. Using GMD, we can decompose the time-domain channel matrix \mathbf{H} into

$$\mathbf{H} = \mathbf{B}_H \mathbf{E}_H \mathbf{P}_H^H, \quad (14)$$

where \mathbf{B}_H and \mathbf{P}_H are unitary matrices while \mathbf{E}_H is a real-valued upper triangular matrix whose diagonal elements equal the geometric mean of the positive singular values of \mathbf{H} , $\|\mathbf{H}^H \mathbf{H}\|^{1/2K}$.

Substituting (14) into (5) and applying QRD to the matrix $[\mathbf{I}_K \otimes \mathbf{w}_n^T] \mathbf{B}_H$, we have

$$\mathbf{H}_n = \mathbf{Q}_{n,B} \mathbf{G}_{n,E} \mathbf{P}_H^H, \quad (15)$$

where $\mathbf{G}_{n,E} = \mathbf{R}_{n,B} \mathbf{E}_H$ is upper triangular. In the sequel, the scheme using (15) is referred to as the QRD/GMD-based precoding scheme (QRD/GMD-PCS). Since (15) is expressed in the same form as (7), discussions on precoding matrix selection and data detection in Sec. III are also applicable to QRD/GMD-PCS.

Albeit the similarity between (15) and GMD, the diagonal elements of $\mathbf{G}_{n,E}$ are no longer guaranteed to be equal due to the latter's dependence on $\mathbf{R}_{n,B}$. Despite such a discrepancy, simulation results shown in the later section indicate that QRD/GMD-PCS can considerably improve BER performance compared to QRD/SVD-PCS.

V. PARTIAL SPATIAL-RATE SYSTEMS

Thus far, we have focused on full-rate MIMO systems with $N_t = N_r = K$. Now, partial spatial-rate systems with $N_t > N_r$ are considered. An immediate advantage of $N_t > N_r$ transmit antennas is the extra spatial degrees of freedom to improve BER performance. The results here on partial-rate systems are also applicable to QRD/GMD-PCS for which detailed discussion is omitted.

To take full advantage of the spatial multiplexing gain, we assume that $K = N_r$ data streams are transmitted from the $N_t > N_r$ elements. We use the superscript $(\cdot)'$ to differentiate the notations in partial spatial-rate systems from their counterparts in full-rate systems. In the former, the frequency response channel matrix corresponding to (5) becomes

$$\mathbf{H}'_n = [\mathbf{I}_{N_r} \otimes \mathbf{w}_n^T] \mathbf{H}', \quad (16)$$

with $\mathbf{H}' \in \mathbb{C}^{N_r N_f \times N_t}$. Repeating the same steps proposed in (7), \mathbf{H}'_n can be decomposed as:

$$\mathbf{H}'_n = \mathbf{Q}'_{n,U} \mathbf{R}'_{n,\Lambda} \mathbf{V}'_{H^H}, \quad (17)$$

with $\mathbf{Q}'_{n,U} \in \mathbb{C}^{N_r \times N_r}$, $\mathbf{R}'_{n,\Lambda} \in \mathbb{C}^{N_r \times N_t}$ and $\mathbf{V}'_{H^H} \in \mathbb{C}^{N_t \times N_t}$.

Recalling $N_t > N_r$, we should choose a precoding matrix $\mathbf{T}'^{(j)}$ containing the N_r columns of \mathbf{V}'_{H^H} associated with the N_r non-zero singular values. Since the design of the soft-QRD-M detector is independent of the precoding matrix dimension, data detection for partial spatial-rate QRD/SVD-PCS can be straightforwardly derived in a similar fashion as shown in Sec. III.

VI. SIMULATION RESULTS

In this section, we assess the performance of the proposed precoded system in terms of coded information bit error rate (BER) and *effective* average throughput using computer simulation. Unlike the conventional throughput definition, the effective average throughput at the decoder output is defined as [9]

$$T_{t-e} \triangleq (1 - \text{BLER}) \times \text{coding-rate} \times N_t \times \text{mod-factor}, \quad (18)$$

where BLER denotes the coded block error rate and “mod-factor” is the symbol modulation order. As shown in [9], the effective average throughput can better characterize the practical capacity by excluding erroneous packets and overheads required for channel coding. For comparison

purposes, we also simulate the performance of SVD-PCS and GMD-PCS. To fairly compare all systems under consideration, no power allocation is performed.

The IEEE 802.11n model D is employed in our experiments with ρ denoting the antenna correlation coefficient [10]. Furthermore, the simulated coded systems adopt a rate-3/4 irregular LDPC code with coding rates being specified in the IEEE 802.11n standard for systems with different antenna configurations [10]. All simulated systems employ soft-QRD-M detectors with $M = 12$ and the Max-Log-MAP algorithm for LDPC decoding. Unless otherwise specified, the data symbols are taken from a QPSK constellation and the DFT size is set to $N = 64$.

A. Full-rate MIMO-OFDM systems with $N_t = N_r = 2$ and $\rho = 0$

Example 1: Performance Comparison with $B = \infty$: Figure 1 shows the information BER performance of SVD-PCS, GMD-PCS, QRD/SVD-PCS and QRD/GMD-PCS as a function of SNR. Inspection of Figure 1 reveals that the proposed QRD/SVD-PCS and QRD/GMD-PCS substantially outperform SVD-PCS by more than 5 dB and 10 dB at BER of 10^{-4} , respectively. This improvement can be better appreciated by observing Figure 2 where the standard deviations of the diagonal elements of Λ_{H_n} in (3), $\mathbf{R}_{n,\Lambda}$ in (7) and $\mathbf{G}_{n,E}$ in (15) are shown as a function of ρ . Figure 2 suggests that the diagonal elements of $\mathbf{G}_{n,E}$ and $\mathbf{R}_{n,\Lambda}$ employed in QRD/GMD-PCS and QRD/SVD-PCS, respectively, have much smaller standard deviations than those of Λ_{H_n} employed in SVD-PCS. Moreover, it is interesting to observe that the standard deviation of the diagonal elements of $\mathbf{G}_{n,E}$ is only marginally affected by the increase of transmit correlation coefficient ρ . From Figure 2, it is easy to understand that the performance of SVD-PCS is actually impaired by the low-SNR spatial subchannels whereas both QRD/SVD-PCS and QRD/GMD-PCS exploit the spatial diversity inherent in the layered subchannels through the soft-QRD-M receiver. Furthermore, QRD/GMD-PCS capitalizes on its GMD operation to effectively distribute transmission power and its performance approaches that of GMD-PCS with perfectly balanced subchannels. Figure 1 indicates that the BER performance degradation of QRD/GMD-PCS with respect to GMD-PCS is only about 0.5 dB at BER of 10^{-4} .

Similar results can be also observed from Figure 3 in which the corresponding effective throughput performance of the four systems is shown. It is clear from Figure 3 that the effective throughput of QRD/SVD-PCS and QRD/GMD-PCS converges to that of GMD-PCS whereas QRD/SVD-PCS achieves more than 80% effective throughput gain over SVD-PCS at SNR of

12 dB.

Example 2: Impact of quantization errors: In the second example, we evaluate a more realistic scenario in which a codebook of finite size 2^B is employed. We repeat the previous experiment at an SNR of 12 dB by evaluating the average throughput for different values of B , yielding Table I. The results of Table I indicate that a quantization level of $B = 6$ bits is sufficient to yield performance close to that with perfect feedback.

	$B = 2$	$B = 4$	$B = 6$	$B = 8$	$B = 10$	$B = \infty$
QRD/SVD-PCS	1.30 bps/Hz	2.33 bps/Hz	2.71 bps/Hz	2.82 bps/Hz	2.84 bps/Hz	2.85 bps/Hz
QRD/GMD-PCS	1.82 bps/Hz	2.59 bps/Hz	2.88 bps/Hz	2.93 bps/Hz	2.93 bps/Hz	2.94 bps/Hz

TABLE I

EFFECTIVE AVERAGE THROUGHPUT ATTAINED WITH CODEBOOKS OF DIFFERENT SIZES.

Example 3: Impact of channel correlation: It is well-known that channel correlation reduces the available spatial degrees of freedom and subsequently degrades the MIMO system performance. Thus, it is important to understand the impact of channel correlation on the overall performance for proposed systems. Figure 4 shows the BER performance of QRD/SVD-PCS and QRD/GMD-PCS as a function of ρ . As ρ increases, the system BER degrades as expected. However, QRD/SVD-PCS is more sensitive to large channel correlation since its subchannel power distribution is directly related to the singular values whereas QRD/GMD-PCS attempts to evenly distribute power over all subchannels by exploiting GMD.

B. Partial spatial-rate MIMO-OFDM systems with $N_t > N_r = 2$ and $\rho = 0.7$

Example 4: Impact of more transmit antennas: For a fixed $N_r = 2$, a larger N_t provides a higher spatial multiplexing gain which is evidenced by Figures. 5 and 6. In Figure 5, the information BER is depicted as a function of N_t at SNR of 15 dB with $N_r = 2$ and $B = \infty$.

VII. CONCLUSION

Two reduced-feedback precoding schemes for MIMO-OFDM systems have been proposed, namely QRD/SVD-PCS and QRD/GMD-PCS. The proposed schemes exploit a novel QRD technique in conjunction with either SVD or GMD that decomposes the MIMO channel into

layered subchannels. In contrast to the conventional precoded MIMO OFDM system, the proposed system employs the same precoding matrix for all carriers. As a result, only one precoding matrix index is required to be returned to the receiver, irrespective of the total number of carriers. Simulation results have confirmed the robust performance of the proposed system.

REFERENCES

- [1] G. G. Raleigh and J. M. Cioffi, "Spatio-temporal coding for wireless communication," *IEEE Trans. Commun.*, vol. 46, pp. 357–366, March 1998.
- [2] Y. Jiang, J. Li, and W. Hager, "Joint transceiver design for MIMO communications using geometric mean decomposition," *IEEE Trans. Signal Processing*, vol. 53, no. 10, pp. 3791–3803, Oct. 2005.
- [3] J. C. Roh and B. D. Rao, "Transmit beamforming in multiple-antenna systems with finite rate feedback: a VQ-based approach," *IEEE Trans. Info. Theory*, vol. 52, pp. 1101–1112, 2006.
- [4] D. J. Love, R. W. Heath Jr., and T. Strohmer, "Grassmannian beamforming for multiple-input multiple-output wireless systems," *IEEE Trans. Info. Theory*, vol. 49, pp. 2735–2747, 2003.
- [5] J. Choi and R. W. Heath Jr., "Interpolation based transmit beamforming for MIMO-OFDM with limited feedback," *IEEE Trans. Signal Processing*, vol. 53, pp. 4125–4135, Dec. 2005.
- [6] Q. Li and X. Lin, "Compact feedback for MIMO-OFDM systems over frequency selective channels," in *Proc. IEEE Vehicular Technology Conference, 2005 Spring*, Stockholm, Sweden, May 2005, pp. 187–191.
- [7] K. J. Kim, T. Reid, and R. A. Iltis, "Iterative Soft-QRD-M for Turbo Coded MIMO-OFDM systems," *IEEE Trans. Commun.*, vol. 56, pp. 1043 – 1046, July 2008.
- [8] X. Wang and H. Poor, "Iterative (turbo) soft interference cancellation and decoding for coded CDMA," *IEEE Trans. Commun.*, vol. 47, pp. 1046–1061, 1999.
- [9] D. Shen, Z. Pan, K. Wong, and V. O. K. Li, "Effective throughput: A unified benchmark for pilot-aided OFDM/SDMA wireless communication systems," in *Proc. Twenty-Second Annual Joint Conference of the IEEE Computer and Communications Societies (INFOCOM 2003)*, San Francisco, USA, March 2003, pp. 1603–1613.
- [10] IEEE P802.11n/D1.04, "Wireless LAN medium access control (MAC) and physical layer (PHY) specifications: Enhancements for higher throughput," September 2006.

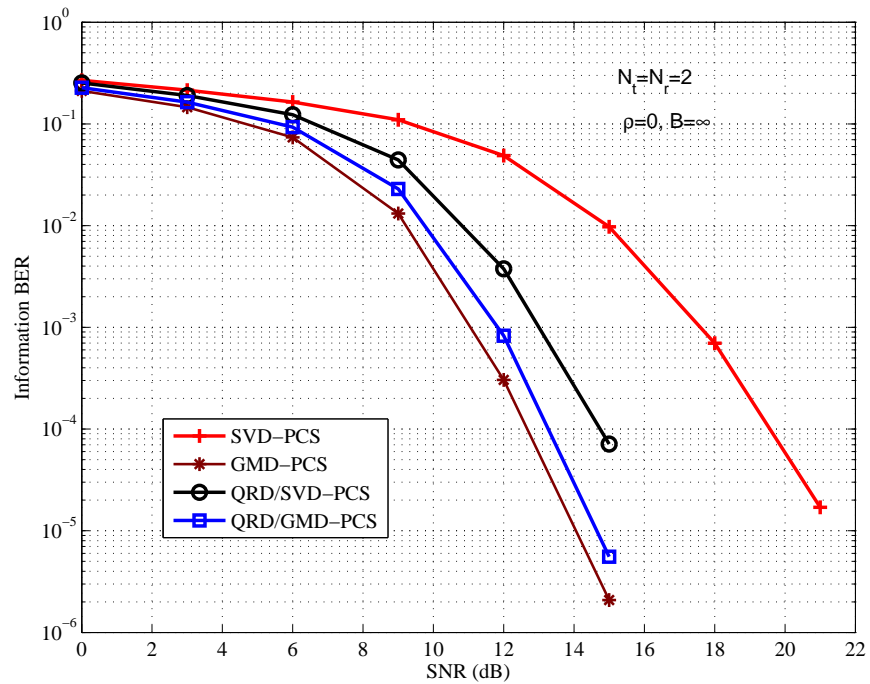


Fig. 1. Information BER performance as a function of SNR with $N_r = N_t = 2$, $\rho = 0$ and $B = \infty$.

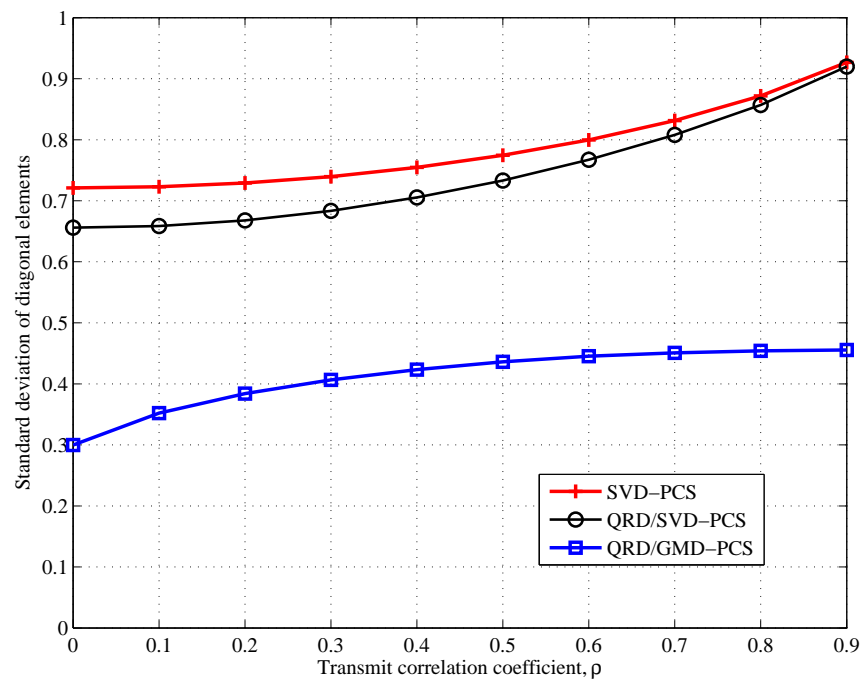


Fig. 2. Standard deviations of the diagonal elements of Λ_{H_n} , $R_{n,\Lambda}$ and $G_{n,E}$ as a function of ρ .

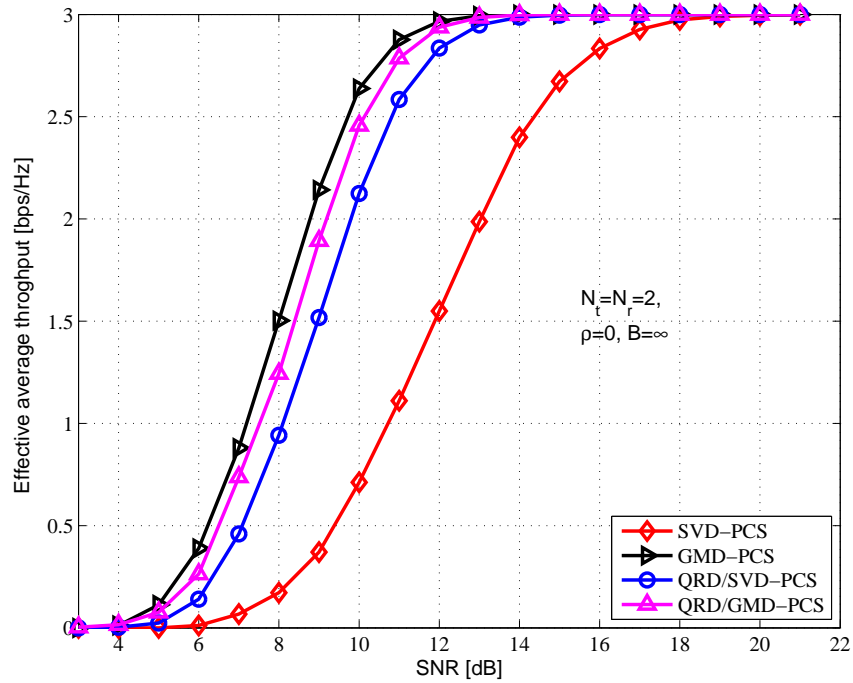


Fig. 3. Effective throughput performance as a function of SNR with $N_r = N_t = 2$, $\rho = 0$ and $B = \infty$.

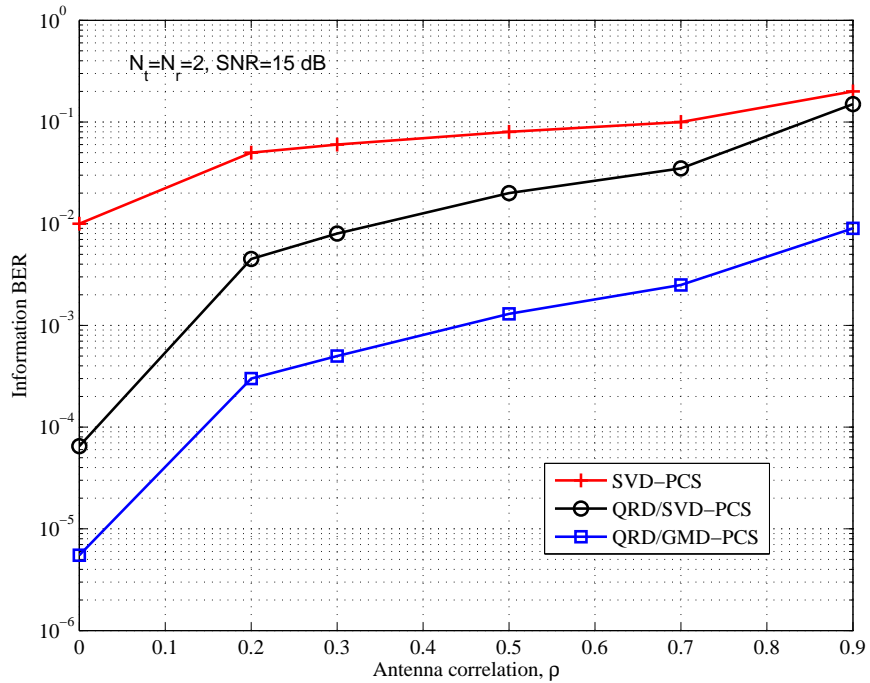


Fig. 4. Information BER performance as a function of ρ at SNR of 15 dB with $N_r = N_t = 2$ and $B = \infty$.

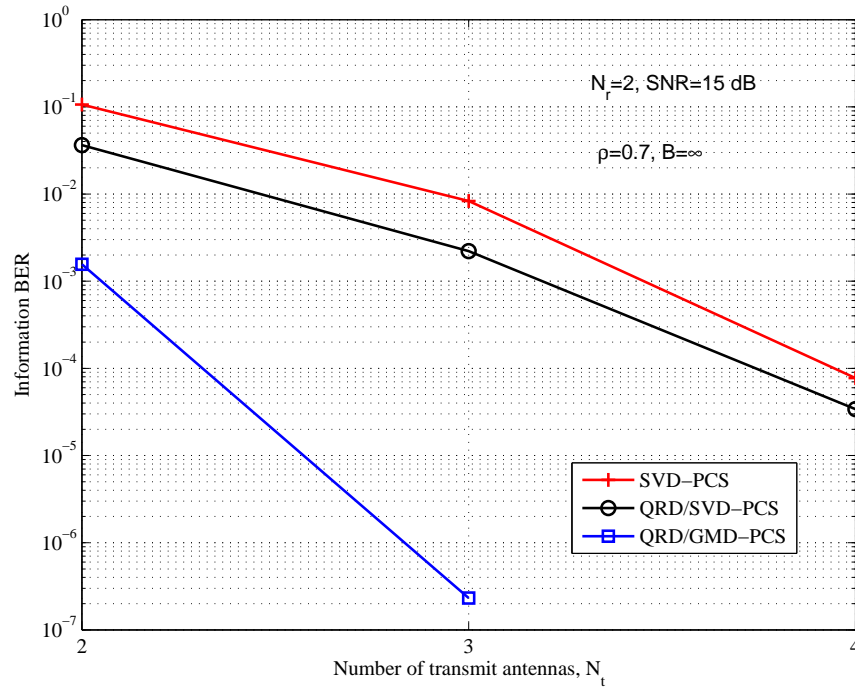


Fig. 5. Information BER performance as a function of N_t at SNR of 15 dB with $N_r = 2$ and $B = \infty$.

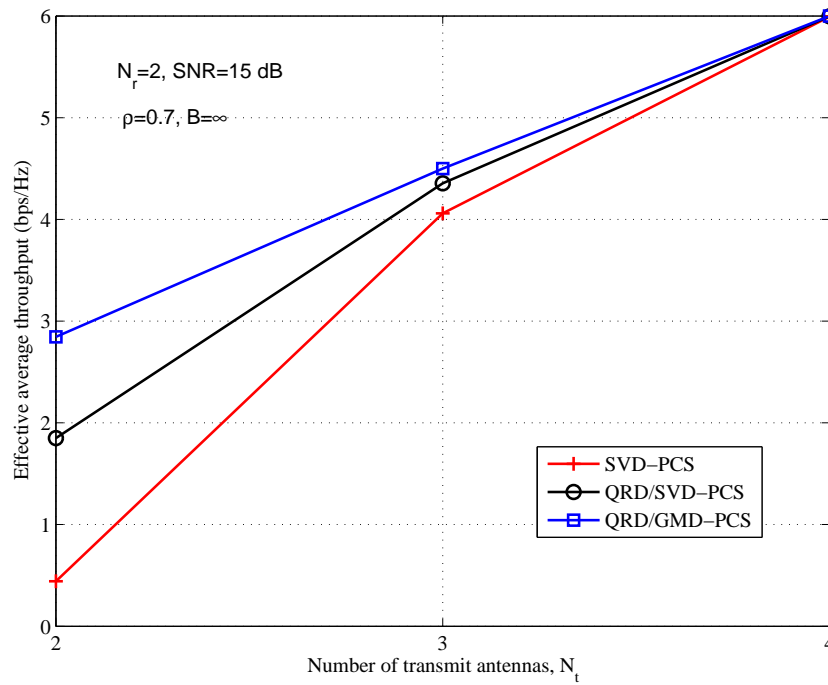


Fig. 6. Effective throughput performance as a function of N_t at SNR of 15 dB with $N_r = 2$ and $B = \infty$.